Future Journal of Pharmaceutical Sciences

RESEARCH

Open Access

Characterization, cellular uptake in Caco-2 cells and physiologically based pharmacokinetic modeling of baicalin-loaded solid lipid nanoparticles

Hussein O. Ammar[1], Rehab N. Shamma[2], Carol Yousry[2], Rasha S. Elbatanony[1], Basma Khater[1] and Amira M. Ghoneim[1*]

Abstract

Background Baicalin is a natural compound having intriguing and useful pharmacological properties that may be used alone or in conjunction with other treatments in a variety of therapeutic areas. However, the drug has low aqueous solubility and poor absorption. The aim of this research was to optimize the bioavailability of baicalin through incorporation into solid lipid nanoparticles.

Results The particle size of the prepared baicalin-loaded solid lipid nanoparticles ranged between 248.2 ± 1.72 nm and 291.9 ± 30.9 nm. The speed, duration of homogenization and the content of both the surfactant and soy lecithin affected the particle size and the entrapment efficiency. The optimized formula showed superiority in drug release over the drug suspension, with biphasic release profile. Cell culture results showed good accumulation of the drug into the Caco-2 cells that increases over time in the case of the optimized formula. Physiologically based pharmacokinetic (PBPK) modeling simulated enhanced bioavailability of the optimized formula, compared to the drug suspension.

Conclusion Solid lipid nanoparticles have demonstrated potential as cancer therapy nanocarriers. Reduced toxicity, improved drug absorption and flexibility in combining hydrophilic and lipophilic medications are all significant advantages of this system. The PBPK simulation suggested the safety of the optimized BA-SLNs in cancer patients and in geriatric populations.

Keywords Baicalin, Solid lipid nanoparticles, Cell culture, PBPK

Background

Scutellariae baicalensis Georgi, often known as Baikal skullcap, has dried roots that may be used to make the glycoside baicalin (BA; baicalein-7-glucuronide). Due to its broad spectrum of therapeutic and preventative potential, BA has lately attracted attention as a safe natural medicinal element [1, 2]. Pharmacologically, BA has an active antibacterial [3], antiviral [4], antifungal [5], anti-inflammatory, antipyretic [6], antihypertensive and antithrombotic effect [7]. BA also acts as a sedative [4, 8] and has antioxidant and hepatoprotective properties [3]. Recently, it has also been noted to have neuroprotective and anticancer properties [9, 10].

Nevertheless, the existence of a glycosyl group on the ring makes BA suffer from first-pass metabolism, poor

*Correspondence:
Amira M. Ghoneim
amiraghoneim@gmail.com
[1] Department of Pharmaceutics and Pharmaceutical Technology, Faculty of Pharmacy, Future University in Egypt, Cairo 11835, Egypt
[2] Department of Pharmaceutics and Industrial Pharmacy, Faculty of Pharmacy, Cairo University, Kasr El-Aini Street, Cairo 12613, Egypt

bioavailability, short half-life and low water solubility [11]. According to the Biopharmaceutics Classification System, it is categorized as a class II medicine with an oral bioavailability as low as 2.2% of the administered dosage [12]. BA had been fabricated into oral chewable tablets, microemulsions, nanoemulsions, self-assembled nanoparticles, nanocrystals, solid dispersions and solid lipid nanoparticles [12–19].

Solid lipid nanoparticles (SLNs), one of the several colloidal carriers now on the market, have varying abilities for the safe formulation of anticancer medications. Solid lipids are used to create SLNs, which has the advantages of other carrier systems. These possible benefits include physical stability, controlled drug release and preservation of vulnerable medicines that are entrapped [18]. SLNs are made from a wide range of lipids, such as glyceride mixes, lipid acids, mono-, di-, or triglycerides or waxes, and the stability is provided by a biocompatible surfactant. The typical particle sizes of SLNs vary from 50 to 1000 nm (s).

Cui et al. [20] worked on boosting oral bioavailability of BA by formulating a carbon mesoporous drug carrier. The results proved that the oral bioavailability of BA was significantly enhanced by the mesoporous carrier. Liu et al. [19] prepared BA solid lipid nanoparticles, using emulsification/ultrasonication method, for ocular delivery, and the results revealed an improvement in the BA bioavailability.

By developing BA-loaded PEGylated nanostructured lipid carriers (BA-PEG-NLC), Zhang et al. [21] aimed to increase BA's bioavailability, extend its in vivo residence duration, and strengthen its protective effect. Their research suggested that PEG-NLC may function as a biocompatible medication delivery system for treating myocardial ischemia. For the manufacture of BA-loaded PEGylated cationic solid lipid nanoparticles, modified by OX26 antibody for brain targeting, Liu et al. [22] used the emulsion evaporation–solidification process. In rats with cerebral ischemia–reperfusion damage, BA absorption across the blood brain barrier and bioavailability in the cerebral spinal fluid were both improved [22].

Shi et al. at [23] prepared BA-loaded NLCs to augment the antidiabetic activity of BA using high-pressure homogenization method. B-NLCs showed a significantly higher antidiabetic efficacy compared with BA plain powder.

The objective of the current study was to present an alternative drug delivery system for BA in the form of SLNs for oral administration in order to improve its therapeutic efficacy and safety as an anticancer drug. The Advanced, Dissolution, Absorption and Metabolism model (ADAM) was utilized for the simulation of BA pharmacokinetic parameters after the oral administration of the optimized BA-loaded NLCs system in adults, geriatrics and cancer patients using Simcyp® Simulator V17.1 software (Certara, Sheffield, UK).

Methods

Materials

Baicalin (BA), soy lecithin (Phospholipon 90G 300G), Roswell Park Memorial Institute Medium (RPMI), trypsin and acetonitrile (HPLC grade) were acquired from Sigma-Aldrich Chemical Co., St. Louis, MO. Stearic acid (SA) was purchased from Mallinckrodt Chemical Works, St. Louis, MO. Tween 80, di-sodium hydrogen phosphate, and sodium di-hydrogen phosphate were obtained from El-Nasr Pharmaceutical Chemicals Co., Cairo, Egypt.

Preparation of solid lipid nanoparticles (SLNs)

SLNs were formulated by an organic solvent-free process which associates the principles of double emulsion and melt dispersion techniques [23, 24] aiming to produce solid lipid particles in the submicron range. Each batch was prepared in triplicate. Stearic acid (0.6 g) was heated beyond its melting point (69.3 °C) and stirred with lecithin. Six milliliters of hot water was mixed with the drug (BA), and the mixture was homogenized for 10 min at 20,000 rpm to form the first emulsion (W1/O). At that time, 6.0 mL of a warm Tween 80 aqueous solution was included to the first emulsion, and the mixture was homogenized for 10 min at 5000 rpm at 25 ± 1 °C by Heidolph homogenizer (Silent Crusher M, Sweden), creating the second emulsion (W1/O/W2). This double emulsion was dispensed into 90.0 mL of cooled water (25 °C) under homogenization for 10 min to support solidification of lipid nanoparticles. As shown in Table 1, the effect of homogenization speed (F1–F3), homogenizing duration (F3–F5), quantity of lecithin (F5–F7), quantity of Tween 80 (F7–F9) and volume of cold water (F9–F11) were investigated.

Particle size analysis, polydispersity index and zeta potential measurements

The particle size (PS), polydispersity index (PDI) and zeta potential (ZP) of SLNs were measured using a Zetasizer 3600 (Malvern Zetasizer Nano series, Worcestershire, UK). Photon correlation spectroscopy at 20 °C without dilution was used for the measurements [25, 26].

Entrapment efficiency

To measure the entrapment efficiency (EE%), drug formulation was centrifuged at − 4 °C, 14.000 rpm (Heraeus Megafuge® 1.0 R; Hanau, Germany), and then, 2 mL of the supernatant was diluted to 10 mL by distilled water. A UV–visible spectrophotometer (UV-1201 Shimadzu,

Table 1 Composition and characterization of the different BA-loaded solid lipid nanoparticles formulations

Formulation	Stearic acid	Soy lecithin	Tween 80	Volume of cold water	Speed of homogenization	Duration of homogenization	PS	PDI	ZP	EE
	(g)	(g)	(g)	(mL)	(rpm)	(min.)	(nm)		(mV)	%
F1	0.6	0.006	0.03	90	20,000	30	260.2 ± 13.5	0.22	− 21.63 ± 2.51	74.06 ± 2.32
F2	0.6	0.006	0.03	90	10,000	30	281.1 ± 9.9	0.25	− 20.85 ± 2.05	72.60 ± 0.69
F3	0.6	0.006	0.03	90	5,000	30	371.1 ± 19.73	0.44	− 23.65 ± 1.20	77.02 ± 1.67
F4	0.6	0.006	0.03	90	20,000	20	248.2 ± 1.70	0.19	− 21.00 ± 1.20	67.80 ± 2.47
F5	0.6	0.006	0.03	90	20,000	10	260.2 ± 23.76	0.22	− 21.63 ± 0.85	76.26 ± 4.24
F6	0.6	0.012	0.03	90	20,000	10	286.6 ± 12.52	0.25	− 22.10 ± 0.14	81.52 ± 0.26
F7	0.6	0.024	0.03	90	20,000	10	288.1 ± 9.05	0.24	− 20.45 ± 0.64	82.75 ± 0.92
F8	0.6	0.024	0.06	90	20,000	10	255.9 ± 20.5	0.18	− 19.20 ± 0.99	76.60 ± 1.41
F9	0.6	0.024	0.12	90	20,000	10	253.5 ± 21.85	0.24	− 18.65 ± 0.50	71.67 ± 0.69
F10	0.9	0.024	0.03	90	20,000	10	292.6 ± 21.85	0.241	− 19.45 ± 0.50	73.00 ± 0.25
F11	1.2	0.024	0.03	90	20,000	10	272.5 ± 12.4	0.22	− 22.50 ± 0.80	70.50 ± 0.50
F12	0.6	0.024	0.06	60	20,000	10	291.9 ± 30.9	0.37	− 19.45 ± 2.62	57.67 ± 5.75
F13	0.6	0.024	0.03	30	20,000	10	286.1 ± 29.96	0.23	− 18.90 ± 2.80	68.09 ± 4.31

PS Particle size, *PDI* Polydispersity index, *ZP* Zeta potential, *EE* Entrapment efficiency

Japan) was used to measure the absorbance of the supernatant dilute measured at 316 nm. The drug entrapped in the formulated SLNs was calculated by subtracting the free drug from the total amount of drug [25]. The EE% was calculated as follows:

$$EE\% = \frac{W_{lp}}{W_{total}} \times 100$$

where W_{lp} = amount of drug entrapped in lipid nanoparticles and W_{total} = total amount of BA. The EE% was determined in triplicates.

In vitro BA release from the SLNs

In vitro drug release study was executed in phosphate buffer pH 6.8 for 4 h. One mL of the formula (containing 0.1 mg of BA) was enclosed in a dialysis bag (cellulose membrane cut off 14,000 mm) and transferred into a beaker holding 50 mL of phosphate buffer at pH 6.8. The beaker was kept in a shaker (Shaker incubator, IKA Ks4000ic, Germany) that was adjusted to 100 horizontal shakes per minute at 37 °C. Three milliliter aliquot of release medium was withdrawn at certain time intervals (0.5, 1, 2, 3 and 4 h) and replenished by the same volume of the buffer. The concentration of the drug in these samples was assessed spectrophotometrically at 316 nm. The study was repeated using 0.1% drug suspension, and all measurements were taken in triplicates.

Transmission electron microscopy

Transmission electron microscopy (TEM, JEOL JEM-1230 TEM, Tokyo, Japan) was used to analyze the morphology of the chosen BA-loaded SLNs at an acceleration voltage of 80 kV. Before TEM observation, one drop of the diluted BA-SLNs was dried on a copper grid that had been coated with carbon, dyed with 2% phosphotungstic acid, and then left to dry at room temperature for 10 min [27, 28].

Cell culture

In order to measure the intracellular uptake of the formulated system, Caco-2 cells suspension was inoculated into a 15-mL culture flask and incubated for 18 h (Dynatech Microplate Reader, MR 5000 Er, West Sussex, UK). On confluency, 1 mL of nanoparticle suspension in RPMI (Roswell Park Memorial Institute Medium) (corresponding to 0.8 µg/mL of BA) was added and cells were re-incubated for variable time intervals (1, 2, 3 and 5 h). After each time interval, the layer of each cell was detached using 1 mL of trypsin and mechanical shaking. One mL of the cell suspension was withdrawn and centrifuged at 4000 rpm for 5 min. The cells were separated and sonicated in 10 µL of acetonitrile to induce cell break. The prepared sample was placed on the ATR (attenuated total reflection) crystal, and its absorbance was measured against BA calibration curve using multiple linear regression. BA solution (containing same concentration of BA) was used as control, where the cellular uptake was measured by assessing the reduction in the BA concentration in the external medium due to the low diffusion of the free drug solution into the cells [29]. The half maximal inhibitory concentration (IC50) was calculated using Master Plex 2010 software.

Physiologically based pharmacokinetic drug input parameters

The physicochemical parameters of BA are displayed in Table 2. Most of these parameters were obtained from data available in the literature [30–32]. The Simcyp® Simulator, a population-based PBPK platform, was used for PBPK modeling (V17.1; Certara, Sheffield, UK). The applied model for BA was the Advanced, Dissolution, Absorption and Metabolism model (ADAM).

Trial design

In vitro data provided the release profile, which was employed as a formulation property for modeling. Three studies were conducted, and each study consisted of ten simulated trials which were performed on 10 healthy male volunteers, $n = 100$ (ages between 20 and 50 years) under fasted conditions to assess the pharmacokinetic (PK) parameters. In all the studies, the dose was set to 10 mg. The simulation was repeated once on 10 geriatric healthy male volunteers (ages between 65 and 75 years) and cancer patients to investigate the influence of age and cancer disease on the PK parameters of the drug.

Table 2 Values of BA parameters for PBPK simulation

Parameters	Value
Molecular weight (g/mol)	446.4
pKa[a]	5.0
Type	Monoprotic acid
Log P[b]	1.2
Fu[c]	0.11
Cl_{int} for CYP1A2 in HLM (µL/min/10^6)[d]	18.3
Km (µM)[e]	52.3
Vmax (pmol//min/10^6)[f]	830.8

[a] Dissociation constants of drug

[b] Partition coefficient

[c] Fraction of drug unbound in plasma

[d] Intrinsic clearance for CYP1A2 in human liver michrosomes

[e] Michaelis–Menten constant

[f] Maximum metabolic rate

Results

Preparation of baicalin-loaded solid lipid nanoparticles (BA-SLNs)

In order to generate solid lipid particles in the submicron dimension; lecithin and Tween 80 were used as surfactants and stearic acid was used as the lipidic material. Lecithin is a well-known wetting and stabilizing agent helping in emulsification and drug encapsulation [33]. Tween 80 is generally present in several products extending from food to pharmaceutical products [33, 34]. It can also be used to prevent aggregation and gelling of lipids in formulation of SLN [35]. The dimensions of the fatty acid chains reflect the hydrophobic nature of the compound, whereas the hydrophilic nature is attained from the ethylene oxide polymers. An increase in the surfactant-particle contact is achieved with high concentration of the surfactant. This encourages surfactant covering of the interface and maintains the SLNs' hydrophobic surfaces during the lipid's polymorphic transition [36, 37]. The hydrocarbon chains in the structure cover the particle, allowing the particle to stay in solution for a longer period of time [36].

Stearic acid has an excellent biodegradability and low toxicity and can be used to incorporate both hydrophilic and lipophilic drugs in nanoparticles [38–40]. The composition of various formulated baicalin-loaded SLNs (BA-SLN) is summarized in Table 1.

Particle size, polydispersity index (PDI) and zeta potential (ZP)

The mean values for the PS, PDI and ZP of the different formulations were determined and are presented in Table 1. PS values of all the formulations varied between 248.2 ± 1.70 nm to 291.9 ± 30.9 nm. The results were statistically analyzed to reveal the independent factors that significantly affect the PS of the prepared BA-loaded SLNs. Statistical analysis revealed that decreasing the homogenization speed from 20,000 rpm (F1) to 10,000 rpm (F2) led to insignificant change in the PS from 260.2 ± 13.5 nm to 281.1 ± 9.9 nm ($p = 0.096$). Further reduction in the speed to 5000 rpm allowed a significant enlargement in PS to 371.05 ± 19.73 nm in F3 ($p < 0.05$). This can be related to the shear force of high intensity, which overcame the intra-forces acting in the particles, resulting in smaller PS. Comparable results were obtained by Kushwaha et al. [41] during the formulation of raloxifene hydrochloride SLNs.

The duration of homogenization was changed from 30 min. (in F1) to 20 min. (in F4), and 10 min. (in F5). The results revealed no significant change in the PS of the obtained BA-loaded SLNs upon changing the homogenization duration ($p > 0.05$), where the PS was 260.2 ± 13.5 nm, 248.2 ± 1.70 nm and 260.2 ± 23.76 nm in F1, F4 and F5, respectively. Therefore, the shortest homogenization duration (10 min.) was selected for further formulations to avoid time consumption.

Finally, the results showed that changing the volume of cold water and the amount of lipid (stearic acid) in the formulation resulted in a non-significant impact on the PS ($p > 0.05$).

The results showed that all prepared SLNs have negatively charged ZP values ranging from − 18.9 ± 2.80 to − 23.65 ± 0.8 mV.

PDI is a function related to the PS of the dispersed SLNs. These values reflect the quality of the dispersion as it ranged from 0 to 1. Table 1 displays the results of PDI values of the prepared BA-loaded SLNs. The results showed that all prepared SLNs have PDI values less than 0.5, indicating monodisperse systems.

Entrapment efficiency (EE%)

Increasing amount of soy lecithin (from 0.006 to 0.012 g) induced a significant rise in EE % of BA ($p < 0.05$) (Table 1). However, further increase in the amount of soy lecithin to 0.024 g did not significantly affect the EE% of BA in the prepared SLNs ($p > 0.05$). The results revealed that other variables, such as changing amount of stearic acid, speed and duration of homogenization and volume of cold water, did not have significant impact on the EE% of BA in the prepared SLNs ($p > 0.05$).

In vitro release

Based on previous results of EE% and particle size, F7 was chosen as the optimum formulation for studying in vitro drug release. Figure 1 exhibits the cumulative amount of BA released versus time profiles for BA-SLNs and BA-suspension.

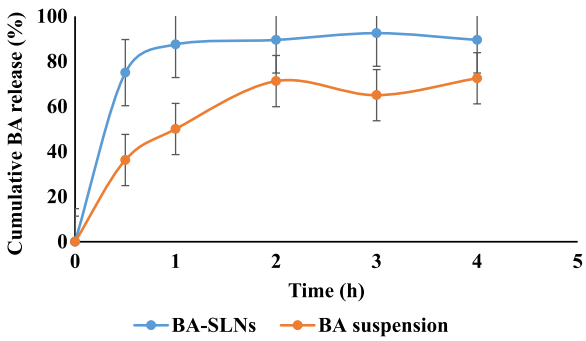

Fig. 1 In vitro release profile of BA from BA-SLNs (F7) and BA-suspension in phosphate buffer pH 6.8

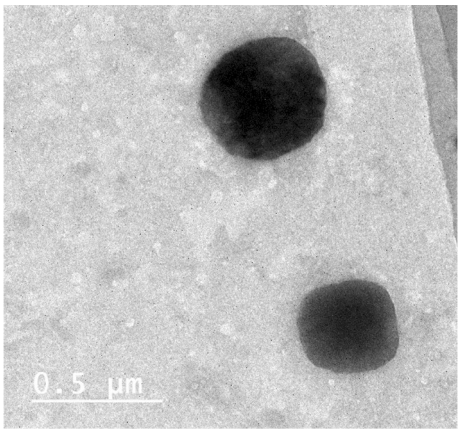

Fig. 2 TEM images of the optimized BA-loaded SLNs (F7)

Transmission electron microscopy (TEM)

TEM images of BA-SLNs are presented in Fig. 2. The images present spherically shaped particles with a smooth surface in the nano-size range with low polydispersity range, where the dark spherical structures are the SLNs. The illustration clearly depicts the particles as smooth spheres, and the sizes of the vesicles shown in the SLNs are consistent with the information gained from the PS analysis.

Cell culture results

The percent viability of BA-SLNs was investigated in vitro on Caco-2 cells. Viability of cells after application of BA-SLNs was analyzed and is demonstrated in Fig. 3. The concentration of BA-SLNs used was in the range of 0.05–50 µg/mL to examine the response of the cells. Surprisingly, the viability of Caco-2 cells was decreased remarkably even at a reduced concentration of SLNs. The toxicity was not substantially enhanced with the different concentrations of BA-SLNs.

Table 3 Mean ± SD of BA pharmacokinetics parameters for BA-suspension and BA-SLNs

Parameters	Treatments	
	BA-suspension	BA-SLNs
T_{max} (h)*	1.98 (1.2–2.5)	1.58 (1.1–2.3)
C_{max}(ng/mL)	288.82 ± 98.90	421.46 ± 136.50
$AUC_{0-24\,h}$ (ng/mL h)	596.77 ± 102.20	1311.09 ± 660.0

*Median (range)

Table 4 Mean ± SD of BA pharmacokinetics parameters for healthy volunteers, geriatrics and cancer patients

Parameters	Healthy volunteers	Geriatrics	Cancer patients
T_{max} (h)*	1.58 (1.1–2.3)	1.93 (1.5–2.7)	1.73 (1.5–2.7)
C_{max} (ng/mL)	421.46 ± 136.50	431.98 ± 98.80	400.85 ± 109.10
$AUC_{0-24\,h}$ (ng/nL h)	1311.09 ± 660.0	1752.16 ± 859.70	1480.79 ± 919.20

*Median (range)

IC50 was calculated and was found to be equivalent to 8.6 µg/mL BA. The results show good accumulation of BA into the Caco-2 cells that increases over time in the case of BA-loaded SLNs. On the other hand, free BA concentration was not varied in the media after the incubation of the cells with BA hydrochloric solution for variable time intervals which reflects poor drug penetration into the cells. These results confirm that SLNs can be a promising vehicle to increase efficacy of BA in cancer therapy.

Analysis of the PBPK model

The PK parameters of BA after oral administration are shown in Tables 3 and 4 and Figs. 4 and 5. A significant difference between the PK behavior of BA-SLNs and

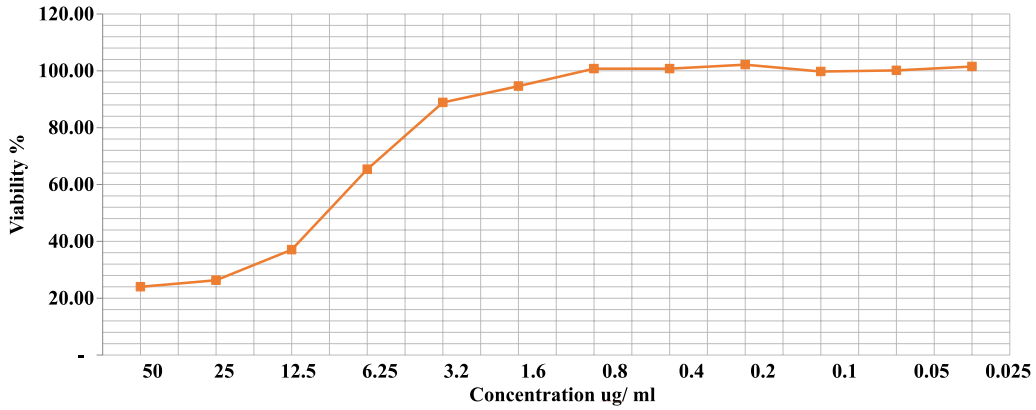

Fig. 3 Cellular uptake of BA-SLNs (F7) into the Caco-2 cells over time

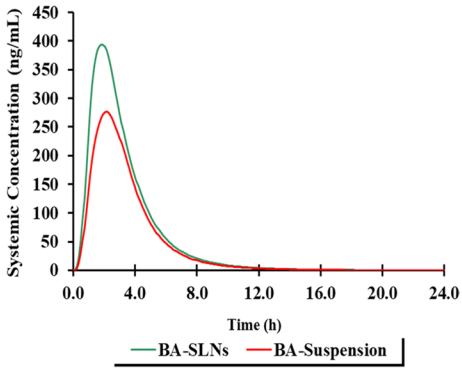

Fig. 4 Mean plasma levels of BA for healthy volunteers in BA-SLNs and BA-suspension

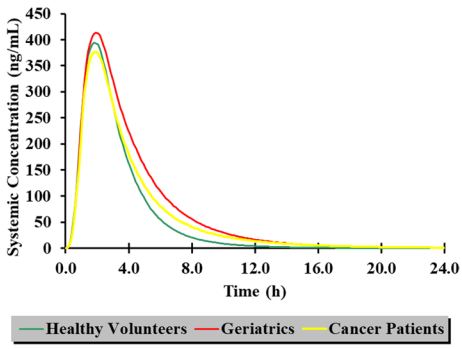

Fig. 5 Mean plasma levels of BA-SLNs for healthy volunteers, geriatrics and cancer patients

BA-suspension was observed. At each time point, the plasma drug concentration of BA-SLNs was much higher than that of BA-suspension. The observed high C_{max} and AUC values following BA-SLNs are in accordance with those described by Hao et al. [42], where BA-SLNs revealed an enhanced oral absorption compared with BA-suspension.

Regarding the pharmacokinetic parameters of the cancer patients receiving BA-SLNs, it can be seen that there is no significant difference between the pharmacokinetic parameters of the cancer patients and healthy volunteers. This shows that BA is safe and tolerable by cancer patients. Unfortunately, very few clinical trials of BA were conducted to study its efficacy for the treatment of tumors in clinics (Scheme 1).

Discussion

Increasing the content of soy lecithin from 0.006 to 0.012 g resulted in a significant increment in the PS of the formulated NPs ($p < 0.05$). Similar outcomes were obtained by Tan et al. [43]. This finding could be related to the capability of soy lecithin to improve the film strength of the formulated NPs, which subsequently increased the percentage of drug encapsulated and, thus, larger SLNs were produced [41]. Further increase in the amount of soy lecithin to 0.024 g resulted in insignificant increase in PS ($p > 0.05$). At high soy lecithin concentration, unstable system consisting of micelles and lamellar aggregates may be formed during the emulsification process. This type of system demonstrates a dynamic process of soy lecithin exchange between the particles [43, 44], which might cause slight rise in the PS.

On the other hand, raising the quantity of Tween 80 from 0.03 to 0.06 g resulted in a non-significant decrease in the PS ($p > 0.05$) of the SLNs. The further addition of the surfactant used in SLNs formulation might lessen the

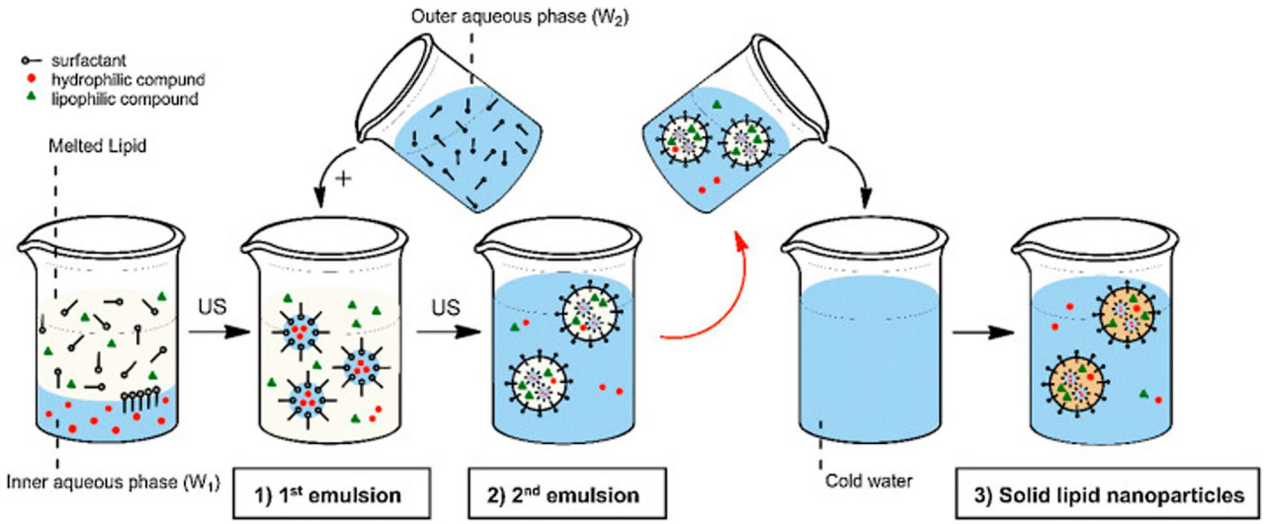

Scheme 1 Schematic representation of the production process of SLNs by double emulsion/melting dispersion

interfacial tension among the lipid matrix and the dispersion medium (aqueous phase), which accordingly favors the development of SLNs with smaller PS. However, the further increase in the amount of Tween 80 to 0.12 g did not show a significant influence on the PS of the formulated SLNs ($p > 0.05$). Similar findings were reported by Thatipamula et al. [45] throughout the formulation of domperidone-loaded SLNs. They suggested that 1.5% of Tween 80 was the optimum concentration to protect the surface of nanoparticles successfully and avoid clustering in the course of the homogenization process.

The surface charges of the SLNs could be accredited to the negatively charged stearic acid used as a lipid [35, 39], in addition to the presence of soy lecithin as surfactant [45]. Although soy lecithin heads are zwitterionic and therefore hypothetically carry no charge at pH 7, they result in negative ZP value in aqueous solution [36, 46]. The development of hydrated layers at the surface and the position of lipid head group [47] can both contribute to this explanation. Makino et al. [48] proposed that the orientation of the dipole linking the opposite charges of the phosphatidyl group and the choline group in the lipid molecule is the cause of the charge of the PC bilayer. It was explained that in low ionic strength medium, the head group is positioned in a way that the phosphatidyl group is facing outward, and the choline group is facing inwards, leading to a negative surface charge [48].

The positive relation between soy lecithin and EE% could be related to the high amount of soy lecithin incorporated, resulting in a greater number of formulated nanoparticles and subsequently a higher quantity of entrapped drug [41]. It is also known that soy lecithin could improve the film strength of the formulated NPs which allows the encapsulation of higher amounts of drug [41]. A study done by Pandita et al. [49] showed that increasing the concentration of surfactants led to an increase in the EE% up to a certain level, where further increase in the surfactant level did not affect the EE% of the formulated NPs. They suggested that excess amount of surfactants may result in flocculation and aggregate formation which may hinder drug encapsulation.

On the other hand, increasing the amount of Tween 80 showed a significant negative impact on the EE% of BA in the prepared SLNs. Van den Bergh et al. [50] reported that raising the surfactant content can cause pores to grow in surface bilayers. Once the concentration of the surfactant reaches a particular level, micelles or mixed micelles are produced, which lowers the EE%.

The in vitro release study demonstrated an initial burst release of BA in phosphate buffer (6.8 pH) up to 1 h (78.5% ± 3.92) and approximately 90% after 4 h. The release of BA from the outer layer of lipid matrix and the surfactant shell of the SLNs could be the reason behind the early burst. The initial rapid release of BA from the SNL could be interpreted by the larger specific surface of the smaller particles. These results suggested that BA-SLNs were able to improve BA release from the formulated SLNs compared to BA aqueous suspension.

This is one way to illustrate how BA-SLNs' biphasic drug release design works: The first burst release may be connected to dual effects through both the rapid release of a little amount of BA that is present in the surface layer of the SLNs and the passive diffusion of BA. Then, with the erosion of SLNs, the release profile up to 4 h may have resulted from the BA incorporated into the inner core of SLNs.

The results of the cell culture study are in agreement with those reported by Chirio et al. [51] when investigating permeability of floxuridine SLNs in cancer therapy. Scholer et al. [52] reported considerable cytotoxic effects when murine peritoneal macrophages cells were treated with SLN incorporating stearic acid or dimethyl dioctadecyl ammonium bromide. Comparable findings were achieved by Marslin et al. [53], where enhanced cytotoxicity of albendazole SLNs was observed compared to that of the free drug due to the efficient uptake of SLNs by the cells. In another study by Wang et al. [54] for preparation of etoposide SLNs for treatment of gastric cancer, an increase in cellular uptake of etoposide SLNs was shown in comparison with that of free drug and it was attributed to the good dispersity and stability of SLNs in an aqueous solution which could facilitate greater cellular uptake compared to free drug. Similar outcomes were also acquired by Xu et al. [55] in preparation of paclitaxel SLNs for treatment of breast cancer. Their results confirmed that SLNs increased the intracellular uptake of drug when compared to the free drug. This enhanced uptake could be attributed to the use of different endocytosis pathways by SLNs in multidrug resistance cells from drug-sensitive cancer cells [56].

Analysis of the PBPK model revealed an increase in oral BA bioavailability which may be due to a number of factors. The particle size presented a principal part in the absorption rate of the nanoparticles. As previously discussed in the in vitro study, the small particle size of BA-SLNs (288.1 ± 9.05 nm) could improve the rate of dissolution by expanding the surface area as stated in the Noyes–Whitney equation; consequently, the improvement in oral bioavailability was inevitable due to the reduced particle size and greater surface area that led to enhanced absorption in the gastrointestinal tract. Furthermore, nanoparticles may be inclined to adhere to mucosal surfaces at the absorption site, thus increasing the absorption and the uptake of BA and avoiding the bypass liver first-pass metabolism [32]. Li et al. [57] reported that the bioavailability of BA was enhanced approximately 2.6

times by solid lipid nanoparticles, which could be attributed to enhanced permeability induced by soy lecithin and Tween 80. Tween 80 renders the surface more hydrophilic, thus improving wettability [58].

Some variations in drug absorption, distribution, biotransformation and elimination are known to occur with aging [54]. The simulation using the pre-existing population of the elderly showed a 30–40% reduction in the GFR for the elderly in contrast to the typical value of 120 mL/min/ 1.73 m^2. Hepatic and renal function reduction and changes in plasma protein concentrations occur with aging [59]. In the older population, decreased hepatic blood flow and impairment in the activity of hepatic CYP enzymes may result in decreased clearance of medications metabolized by the liver [59]. It is evident that there is a slight increase in the pharmacokinetic parameters of the geriatrics compared to healthy volunteers. This could be due to BA being subjected to extensive metabolism, via conjugative reactions, in the intestinal regions.

Conclusion

Solid lipid nanoparticles (SLNs) have shown promise as nanocarriers for the treatment of cancer. Significant benefits that SLNs offer include decreased toxicity, increased medicine bioavailability, and flexibility in integrating hydrophilic and lipophilic pharmaceuticals. These particles' nano-sizes enable them to pass through a variety of biological barriers and deliver medications to the areas of action with minimal toxicity [60]. In addition to the advantages listed above, the use of SLNs in anticancer therapy may also enable oral medicine administration and lengthen the duration that cancer cells are exposed to pharmaceuticals as compared to other delivery methods. This can imply the usage of simpler and more suited treatments for the patients. SLNs provide primarily competent drug delivery methods for the advancement of cancer chemotherapeutic treatments, taking into account the impact of cancer on people all over the world and the need for more effective pharmaceuticals. Many studies are increasingly using PBPK modeling to provide mechanistic predictions of pharmacokinetics and disposal in a variety of populations and dosing regimens. The methods for creating models and determining their level of quality, however, vary considerably. The PBPK simulation suggested the safety of the optimized BA-SLNs in cancer patients and in geriatric populations.

Abbreviations

ADAM	Advanced, Dissolution, Absorption and Metabolism model
BA	Baicalein-7-glucuronide
BA-PEG-NLC	BA-loaded PEGylated nanostructured lipid carriers
EE%	Entrapment efficiency
PBPK	Physiologically based pharmacokinetic modeling
PDI	Polydispersity index
PK	Pharmacokinetic
PS	Particle size
SA	Stearic acid
SLNs	Solid lipid nanoparticles
TEM	Transmission electron microscopy
ZP	Zeta potential

Acknowledgements
Not applicable.

Author contributions
HOA and RNS were involved in conception and design of the work. CY and BK analyzed and interpreted the data. AG and RE wrote and revised the work.

Funding
The authors received no funding.

Availability of data and materials
Data are available upon request.

Declarations

Ethics approval and consent to participate
Not applicable.

Consent for publication
Not applicable.

Competing interests
The authors declare that they have no competing interests.

Received: 12 April 2023 Accepted: 11 July 2023
Published online: 31 July 2023

References

1. Li C, Lin G, Zuo Z (2011) Pharmacological effects and pharmacokinetics properties of Radix Scutellariae and its bioactive flavones. Biopharm Drug Dispos 32(8):427–445. https://doi.org/10.1002/bdd.771
2. Wu S, Sun A, Liu R (2005) Separation and purification of baicalin and wogonoside from the Chinese medicinal plant *Scutellaria baicalensis* Georgi by high-speed counter-current chromatography. J Chromatogr A 1066(1–2):243–247. https://doi.org/10.1016/j.chroma.2005.01.054
3. Luo J, Dong B, Wang K, Cai S, Liu T, Cheng X, Lei D, Chen Y, Li Y, Kong J, Chen Y (2017) Baicalin inhibits biofilm formation, attenuates the quorum sensing-controlled virulence and enhances *Pseudomonas aeruginosa* clearance in a mouse peritoneal implant infection model. PLoS One 12(4):e0176883. https://doi.org/10.1371/journal.pone.0176883
4. Huang H, Zhou W, Zhu H, Zhou P, Shi X (2017) Baicalin benefits the anti-HBV therapy via inhibiting HBV viral RNAs. Toxicol Appl Pharmacol 15(323):36–43. https://doi.org/10.1016/j.taap.2017.03.016
5. Wang T, Shi G, Shao J, Wu D, Yan Y, Zhang M, Cui Y, Wang C (2015) In vitro antifungal activity of baicalin against *Candida albicans* biofilms via apoptotic induction. Microb Pathog 87:21–29. https://doi.org/10.1016/j.micpath.2015.07.006
6. Lee W, Ku SK, Bae JS (2015) Anti-inflammatory effects of Baicalin, Baicalein, and Wogonin in vitro and in vivo. Inflammation 38(1):110–125. https://doi.org/10.1007/s10753-014-0013-0
7. Deng YF, Aluko RE, Jin Q, Zhang Y, Yuan LJ (2012) Inhibitory activities of baicalin against renin and angiotensin-converting enzyme. Pharm Biol 50(4):401–406. https://doi.org/10.3109/13880209.2011.608076
8. Xu Z, Wang F, Tsang SY, Ho KH, Zheng H, Yuen CT, Chow CY, Xue H (2006) Anxiolytic-like effect of baicalin and its additivity with other anxiolytics. Planta Med 72(2):189–192. https://doi.org/10.1055/s-2005-873193
9. Liao CC, Day YJ, Lee HC, Liou JT, Chou AH, Liu FC (2016) Baicalin attenuates IL-17-mediated acetaminophen-induced liver injury in a mouse

model. PLoS One 11(11):e0166856. https://doi.org/10.1371/journal.pone.0166856
10. Gong WY, Zhao ZX, Liu BJ, Lu LW, Dong JC (2017) Exploring the chemopreventive properties and perspectives of baicalin and its aglycone baicalein in solid tumors. Eur J Med Chem 126:844–852. https://doi.org/10.1016/j.ejmech.2016.11.058
11. Liu X, Gu J, Fan Y, Shi H, Jiang M (2013) Baicalin attenuates acute myocardial infarction of rats via mediating the mitogen-activated protein kinase pathway. Biol Pharm Bull 36(6):988–994. https://doi.org/10.1248/bpb.b13-00021
12. Wang W, Xi M, Duan X, Wang Y, Kong F (2015) Delivery of baicalein and paclitaxel using self-assembled nanoparticles: synergistic antitumor effect in vitro and in vivo. Int J Nanomed 10:3737–3750. https://doi.org/10.2147/IJN.S80297
13. Zhang J, Lv H, Jiang K, Gao Y (2011) Enhanced bioavailability after oral and pulmonary administration of baicalein nanocrystal. Int J Pharm 420(1):180–188. https://doi.org/10.1016/j.ijpharm.2011.08.023
14. Xing J, Chen X, Zhong D (2005) Absorption and enterohepatic circulation of baicalin in rats. Life Sci 78(2):140–146. https://doi.org/10.1016/j.lfs.2005.04.072
15. Li M, Shi A, Pang H, Xue W, Li Y, Cao G, Yan B, Dong F, Li K, Xiao W, He G, Du G, Hu X (2014) Safety, tolerability, and pharmacokinetics of a single ascending dose of baicalein chewable tablets in healthy subjects. J Ethnopharmacol 156:210–215. https://doi.org/10.1016/j.jep.2014.08.031
16. He X, Pei L, Tong HH, Zheng Y (2011) Comparison of spray freeze drying and the solvent evaporation method for preparing solid dispersions of baicalein with Pluronic F68 to improve dissolution and oral bioavailability. AAPS PharmSciTech 12(1):104–113. https://doi.org/10.1208/s12249-010-9560-3
17. Mu H, Holm R (2018) Solid lipid nanocarriers in drug delivery: characterization and design. Expert Opin Drug Deliv 15(8):771–785. https://doi.org/10.1080/17425247.2018.1504018
18. Wissing SA, Kayser O, Müller RH (2004) Solid lipid nanoparticles for parenteral drug delivery. Adv Drug Deliv Rev 56(9):1257–1272. https://doi.org/10.1016/j.addr.2003.12.002
19. Liu Z, Zhao H, Shu L, Zhang Y, Okeke C, Zhang L, Li J, Li N (2015) Preparation and evaluation of Baicalin-loaded cationic solid lipid nanoparticles conjugated with OX26 for improved delivery across the BBB. Drug Dev Ind Pharm 41(3):353–361. https://doi.org/10.3109/03639045.2013.861478
20. Cui L, Sune E, Song J, Wang J, Jia XB, Zhang ZH (2016) Characterization and bioavailability study of baicalin-mesoporous carbon nanopowder solid dispersion. Pharmacogn Mag 12(48):326–332. https://doi.org/10.4103/0973-1296.192199
21. Zhang S, Wang J, Pan J (2016) Baicalin-loaded PEGylated lipid nanoparticles: characterization, pharmacokinetics, and protective effects on acute myocardial ischemia in rats. Drug Deliv 23(9):3696–3703. https://doi.org/10.1080/10717544.2016.1223218
22. Liu Z, Zhang L, He Q, Liu X, Okeke CI, Tong L, Guo L, Yang H, Zhang Q, Zhao H, Gu X (2015) Effect of Baicalin-loaded PEGylated cationic solid lipid nanoparticles modified by OX26 antibody on regulating the levels of baicalin and amino acids during cerebral ischemia-reperfusion in rats. Int J Pharm 489(1–2):131–138. https://doi.org/10.1016/j.ijpharm.2015.04.049
23. Shi F, Wei Z, Zhao Y, Xu X (2016) Nanostructured lipid carriers loaded with baicalin: an efficient carrier for enhanced antidiabetic effects. Pharmacogn Mag 12(47):198–202. https://doi.org/10.4103/0973-1296.186347
24. Bodmeier R, Wang J, Bhagwatwar H (1992) Process and formulation variables in the preparation of wax microparticles by a melt dispersion technique. I. Oil-in-water technique for water-insoluble drugs. J Microencapsul 9(1):89–98. https://doi.org/10.3109/02652049209021226
25. Reithmeier H, Herrmann J, Göpferich A (2001) Lipid microparticles as a parenteral controlled release device for peptides. J Control Release 73(2–3):339–350. https://doi.org/10.1016/s0168-3659(01)00354-6
26. Elshall AA, Ghoneim AM, Abdel-Mageed HM, Osman R, Shaker DS (2022) Ex vivo permeation parameters and skin deposition of melatonin-loaded microemulsion for treatment of alopecia. Futur J Pharm Sci 8:28. https://doi.org/10.1186/s43094-022-00418-4
27. Abdel-Salam FS, Elkheshen SA, Mahmoud AA, Ammar HO (2015) Diflucortolone valerate loaded solid lipid nanoparticles as a semisolid topical delivery system. Bull Fac Pharm Cairo Univ 54(1):1–7. https://doi.org/10.1016/j.bfopcu.2015.11.002
28. Ammar HO, Tadros MI, Salama NM, Ghoneim AM (2020) Ethosome-derived invasomes as a potential transdermal delivery system for vardenafil hydrochloride: development, optimization and application of physiologically based pharmacokinetic modeling in adults and geriatrics. Int J Nanomed 15:5671–5685. https://doi.org/10.2147/IJN.S261764
29. Joshi G, Kumar A, Sawant K (2016) Bioavailability enhancement, Caco-2 cells uptake and intestinal transport of orally administered lopinavir-loaded PLGA nanoparticles. Drug Deliv 23(9):3492–3504. https://doi.org/10.1080/10717544.2016.1199605
30. Jakab G, Bogdán D, Mazák K, Deme R, Mucsi Z, Mándity IM, Noszál B, Kállai-Szabó N, Antal I (2019) Physicochemical profiling of baicalin along with the development and characterization of cyclodextrin inclusion complexes. AAPS PharmSciTech 20:314. https://doi.org/10.1208/s12249-019-1525-6
31. Wang W, Zheng B, Wu J, Lv W, Lin P, Gong X (2021) Determination of the dissociation constants of 16 active ingredients in medicinal herbs using a liquid-liquid equilibrium method. Separations 8:49. https://doi.org/10.3390/separations8040049
32. Gao N, Qi B, Liu FJ, Fang Y, Zhou J, Jia LJ, Qiao HL (2014) Inhibition of baicalin on metabolism of phenacetin, a probe of CYP1A2, in human liver microsomes and in rats. PLoS One 9(2):e89752. https://doi.org/10.1371/journal.pone.0089752
33. Bose S, Du Y, Takhistov P, Michniak-Kohn B (2013) Formulation optimization and topical delivery of quercetin from solid lipid based nanosystems. Int J Pharm 441(1–2):56–66. https://doi.org/10.1016/j.ijpharm.2012.12.013
34. Helgason T, Awad TS, Kristbergsson K, McClements DJ, Weiss J (2009) Effect of surfactant surface coverage on formation of solid lipid nanoparticles (SLN). J Colloid Interface Sci 334(1):75–81. https://doi.org/10.1016/j.jcis.2009.03.012
35. del Pozo-Rodríguez A, Delgado D, Solinís MA, Gascón AR, Pedraz JL (2007) Solid lipid nanoparticles: formulation factors affecting cell transfection capacity. Int J Pharm 339(1–2):261–268. https://doi.org/10.1016/j.ijpharm.2007.03.015
36. Kim BD, Na K, Choi HK (2005) Preparation and characterization of solid lipid nanoparticles (SLN) made of cacao butter and curdlan. Eur J Pharm Sci 24(2–3):199–205. https://doi.org/10.1016/j.ejps.2004.10.008
37. Yang Y, Corona A, Schubert B, Reeder R, Henson MA (2014) The effect of oil type on the aggregation stability of nanostructured lipid carriers. J Colloid Interface Sci 418:261–272
38. Ezzati Nazhad Dolatabadi J, Hamishehkar H, Eskandani M, Valizadeh H (2014) Formulation, characterization and cytotoxicity studies of alendronate sodium-loaded solid lipid nanoparticles. Colloids Surf B Biointerfaces 117:21–28. https://doi.org/10.1016/j.colsurfb.2014.01.055
39. Becker Peres L, Becker Peres L, de Araújo PHH, Sayer C (2016) Solid lipid nanoparticles for encapsulation of hydrophilic drugs by an organic solvent free double emulsion technique. Colloids Surf B Biointerfaces 140:317–323. https://doi.org/10.1016/j.colsurfb.2015.12.033
40. Paliwal R, Rai S, Vaidya B, Khatri K, Goyal AK, Mishra N, Mehta A, Vyas SP (2009) Effect of lipid core material on characteristics of solid lipid nanoparticles designed for oral lymphatic delivery. Nanomedicine 5(2):184–191. https://doi.org/10.1016/j.nano.2008.08.003
41. Kushwaha AK, Vuddanda PR, Karunanidhi P, Singh SK, Singh S (2013) Development and evaluation of solid lipid nanoparticles of raloxifene hydrochloride for enhanced bioavailability. Biomed Res Int 2013:584549. https://doi.org/10.1155/2013/584549
42. Hao J, Wang F, Wang X, Zhang D, Bi Y, Gao Y, Zhao X, Zhang Q (2012) Development and optimization of baicalin-loaded solid lipid nanoparticles prepared by coacervation method using central composite design. Eur J Pharm Sci 47(2):497–505. https://doi.org/10.1016/j.ejps.2012.07.006
43. Tan ME, He CH, Jiang W, Zeng C, Yu N, Huang W, Gao ZG, Xing JG (2017) Development of solid lipid nanoparticles containing total flavonoid extract from *Dracocephalum moldavica* L. and their therapeutic effect against myocardial ischemia-reperfusion injury in rats. Int J Nanomed 12:3253–3265. https://doi.org/10.2147/IJN.S131893
44. Loo Ch, Basri M, Ismail R, Lau H, Tejo B, Kanthimathi M, Hassan H, Choo Y (2013) Effect of compositions in nanostructured lipid carriers (NLC) on skin hydration and occlusion. Int J Nanomed 8:13–22. https://doi.org/10.2147/IJN.S35648
45. Thatipamula R, Palem C, Gannu R, Mudragada S, Yamsani M (2011) Formulation and in vitro characterization of domperidone loaded solid lipid nanoparticles and nanostructured lipid carriers. Daru 19(1):23–32

46. Paliwal R, Rai S, Vaidya B, Khatri K, Goyal AK, Mishra N, Mehta A, Vyas SP (2009) Effect of lipid core material on characteristics of solid lipid nanoparticles designed for oral lymphatic delivery. Nanomedicine 5(2):184–191. https://doi.org/10.1016/j.nano.2008.08.003
47. Nandini PT, Doijad RC, Shivakumar HN, Dandagi PM (2015) Formulation and evaluation of gemcitabine-loaded solid lipid nanoparticles. Drug Deliv 22(5):647–651. https://doi.org/10.3109/10717544.2013.860502
48. Makino K, Yamada T, Kimura M, Oka T, Ohshima H, Kondo T (1991) Temperature- and ionic strength-induced conformational changes in the lipid head group region of liposomes as suggested by zeta potential data. Biophys Chem 41(2):175–183. https://doi.org/10.1016/0301-4622(91)80017-l
49. Pandita D, Ahuja A, Velpandian T, Lather V, Dutta T, Khar RK (2009) Characterization and in vitro assessment of paclitaxel loaded lipid nanoparticles formulated using modified solvent injection technique. Pharmazie 64(5):301–310
50. van den Bergh BA, Bouwstra JA, Junginger HE, Wertz PW (1999) Elasticity of vesicles affects hairless mouse skin structure and permeability. J Control Release 62(3):367–379. https://doi.org/10.1016/s0168-3659(99)00168-6
51. Chirio D, Peira E, Battaglia L, Ferrara B, Barge A, Sapino S, Giordano S, Dianzani C, Gallarate M (2018) Lipophilic prodrug of floxuridine loaded into solid lipid nanoparticles: in vitro cytotoxicity studies on different human cancer cell lines. J Nanosci Nanotechnol 18(1):556–563. https://doi.org/10.1166/jnn.2018.13964
52. Schöler N, Hahn H, Müller RH, Liesenfeld O (2002) Effect of lipid matrix and size of solid lipid nanoparticles (SLN) on the viability and cytokine production of macrophages. Int J Pharm 231(2):167–176. https://doi.org/10.1016/s0378-5173(01)00882-1
53. Marslin G, Siram K, Liu X, Khandelwal VKM, Xiaolei S, Xiang W, Franklin G (2017) Solid lipid nanoparticles of albendazole for enhancing cellular uptake and cytotoxicity against U-87 MG glioma cell lines. Molecules 22(11):2040. https://doi.org/10.3390/molecules22112040
54. Gareri P, De Fazio P, Russo E, Marigliano N, De Fazio S, De Sarro G (2008) The safety of clozapine in the elderly. Expert Opin Drug Saf 7(5):525–538. https://doi.org/10.1517/14740338.7.5.525
55. Xu W, Bae EJ, Lee MK (2018) Enhanced anticancer activity and intracellular uptake of paclitaxel-containing solid lipid nanoparticles in multidrug-resistant breast cancer cells. Int J Nanomedicine 13:7549–7563. https://doi.org/10.2147/IJN.S182621
56. Wang J, Zhu R, Sun X, Zhu Y, Liu H, Wang SL (2014) Intracellular uptake of etoposide-loaded solid lipid nanoparticles induces an enhancing inhibitory effect on gastric cancer through mitochondria-mediated apoptosis pathway. Int J Nanomed 9:3987–3998. https://doi.org/10.2147/IJN.S64103
57. Liu Z, Zhang X, Wu H, Li J, Shu L, Liu R, Li L, Li N (2011) Preparation and evaluation of solid lipid nanoparticles of baicalin for ocular drug delivery system in vitro and in vivo. Drug Dev Ind Pharm 37(4):475–481. https://doi.org/10.3109/03639045.2010.522193
58. des Rieux A, Fievez V, Garinot M, Schneider YJ, Préat V (2006) Nanoparticles as potential oral delivery systems of proteins and vaccines: a mechanistic approach. J Control Release 116(1):1–27. https://doi.org/10.1016/j.jconrel.2006.08.013
59. Ghoneim AM, Mansour SM (2020) The effect of liver and kidney disease on the pharmacokinetics of clozapine and sildenafil: a physiologically based pharmacokinetic modeling. Drug Des Devel Ther 14:1469–1479. https://doi.org/10.2147/DDDT.S246229
60. Kaur S, Greaves P, Cooke DN, Edwards R, Steward WP, Gescher AJ, Marczylo TH (2007) Breast cancer prevention by green tea catechins and black tea theaflavins in the C3(1) SV40 T, t antigen transgenic mouse model is accompanied by increased apoptosis and a decrease in oxidative DNA adducts. J Agric Food Chem 55(9):3378–3385. https://doi.org/10.1021/jf0633342

Publisher's Note